Chapter 15

Biomedical Engineering in Epidural Anaesthesia Research

Venketesh N. Dubey, Neil Vaughan,
Michael Y. K. Wee and Richard Isaacs

Additional information is available at the end of the chapter

http://dx.doi.org/10.5772/50764

1. Introduction

The application of engineering techniques into biomedical procedures has proved extremely beneficial in many areas of medicine. A developing area is in epidural analgesia and anaesthesia, a technique employed for the relief of pain in both acute and chronic, and for anaesthesia to enable pain-free surgery. The aim of this chapter is to demonstrate several specific areas of research and how biomedical engineering techniques are used to improve and enhance the experience and training in the epidural procedure. The overall goal is to reduce the risks and subsequent morbidity in patients using advanced technologies to recreate the epidural procedure replicating as far as possible the in-vivo procedure. This would allow anaesthetists to practice the procedure in a safe and controlled environment without risk to patients. This could be achieved by recreating the sensation of the needle passing through the tissues and ligaments and by the generation of forces that match exactly those felt in-vivo. Epidural simulators are currently used as a training aid for anaesthetists, however existing simulators lack realism to various degrees and their operation is not based on measured in-vivo data that can accurately simulate the procedure. The techniques of advanced simulation and biomedical engineering detailed in this chapter can provide a solution.

Haptic devices have been used previously to reproduce needle forces but the forces are often not based on measured data. Needle insertion forces in-vivo are largely unknown as there are few studies in this specific area. Without accurate measurement of resultant pressure on the syringe plunger of the epidural needle, as the needle passes through the various ligaments and tissues of the spine, it is difficult to create accurate simulation of the epidural procedure. The ideal model would require other features such as a palpable spine, ability to accommodate for patient variation, 3D graphics visualisation and an adjustable needle insertion point. Techniques in biomedical engineering can provide solutions through

the design of devices capable of making precise measurements and utilising them in a novel high fidelity epidural simulator. Adequate training on an advanced simulator will help alleviate the risks of epidural failures from inaccurate placement and also reduce potential morbidity to patients thereby improving the safety of the procedure.

This chapter is laid out in various sections to illustrate different aspects of current epidural anaesthesia research. Section 2 describes the actual epidural procedure and its challenges. Section 3 discusses the needle insertion forces in epidurals. Section 4 describes an interspinous pressure measurement device for wireless data collection during needle insertion leading to a porcine trial discussed in Section 5. Section 6 describes an image processing technique for non-contact needle depth measurement that could be used in conjunction with pressure measurement for fully characterising the needle insertion. In Section 7, 3D-modelling of spine with bending and flexing is discussed for flexibility of patient's positions together with heterogeneous volumetric modelling of spinal ligaments in Section 8. Stereo 3D visualisation for depth perception of epidural procedure has been discussed in Section 9. Section 10 applies a haptic force feedback device configured with the measured force data to create an electronic human–computer interface which is described in Section 11. Finally, section 12 brings all these technologies together and demonstrates the complete system that makes up our current epidural simulator prototype with conclusions provided in section 13.

2. Epidural procedure and challenges of clinical simulation

Epidural analgesia and anaesthesia is commonly used as a form of pain relief during childbirth, for the treatment of chronic back pain or as a means to provide anaesthesia or analgesia during specific operations. Monitoring the depth of the needle during an epidural insertion is crucial because once the needle tip enters the epidural space, an epidural catheter is usually sited to a specific length. This enables the intermittent or continuous use of the epidural for anaesthesia or pain relief. If the needle is advanced too far it will puncture the dural sac and cause leakage of cerebrospinal fluid. Post dural puncture headaches may result, which can be extremely disabling for the patient. Other potential risks include nerve damage or bleeding which may very rarely lead to paralysis. If the needle is not within the epidural space, the analgesia or anaesthesia may be ineffective or absent due to incorrect placement of the catheter.

During an epidural insertion, the operator tries to perceive which tissue layer the needle tip is passing through by feeling the resistances on the needle. This is a process known as "haptic" feedback. A simulator can assist the development of this visuospatial awareness of spinal anatomy and 'feel' of the procedure to allow practice prior to attempts on patients. Not only will this serve to enhance patient safety but it also creates a safe and controlled environment in which to learn.

The procedure of inserting an epidural needle into the lumbar spine requires the operator to visualise in their mind a three-dimensional (3D) anatomical image of the bony alignments and the various tissue layers from skin, through to subcutaneous fat, supraspinous and

interspinous ligaments, ligamentum flavum and then to the epidural space. Epidural needle insertion is essentially a blind procedure, but utilises a well-known technique referred to as "loss of resistance" (LOR). LOR essentially involves identification of the epidural space by compression of either fluid or air as the epidural needle encounters the various ligaments of the lumbar vertebral column [1]. Initially, the back of the patient is palpated, and using surface landmarks such as the iliac crests, an assessment is made of suitable intervertebral spaces and of midline. For lumbar epidurals, this may be between lumbar vertebra 3 (L3) and lumbar vertebra 4 (L4) for instance. The epidural or Tuohy needle, as it is commonly called, is inserted into the interspinous ligament and a syringe filled with saline is attached to the end of the needle. These LOR syringes are specially manufactured so that there is less friction between the plunger and the inner wall of the LOR syringe. A constant or intermittent force is then applied to the plunger by the operator's thumb as the needle is slowly advanced forward. As the tougher and more fibrous ligamentum flavum is encountered, a higher resistive force to injection is encountered. Once the needle tip traverses the ligamentum flavum, the epidural space is then entered into and saline can be quite easily injected, hence the phenomenon of LOR. It is this haptic perception that informs the operator of needle location within the various tissue layers, obstruction from bone and loss of resistance from potential spaces such as those between the ligaments. Combining this with the creation in one's mind of a three-dimensional image of lumbar spinal anatomy enables successful placement of an epidural catheter.

The ideal epidural simulator should be capable of replicating the above procedure and aim to recreate as far as possible the in-vivo procedure. A real Tuohy needle could be inserted at any intervertebral space in the lumbar or thoracic region using the midline or paramedian approach [2]. It would contain a force feedback haptic device, with force data originating from measured Tuohy needle insertions from patients. Using measured in-vivo data from patients and integrating this into the epidural simulator software, the resistance would automatically adjust to give patient variation on weight, height and body shape. This could simulate random patients or match measurements from a specific patient. The 3D virtual patient and virtual vertebrae can also be adjusted in size and shape to match measurements from actual patients. As the needle advances, the resultant force should represent each tissue layer and a LOR on reaching the epidural space. Once the epidural space is reached, saline would be released. During the entire insertion, a 3D virtual spine could be displayed on the monitor showing the trajectory of the needle in real time. The manikin could bend forwards to mimic spinal flexion to increase spacing between the vertebrae or alternatively bend backwards (extension) to simulate increased difficulty in locating the interspinous space for training purposes.

Variation in patient size, height, weight and other characteristics should be possible based upon actual patient measurements. Currently, most simulators have only two or three options such as obese, elderly and normal [3-6] which is perhaps not enough to encapsulate reality and could therefore be improved. Simulators could have unlimited patient variation by including parameters such as height, weight, body shape, age, obesity which could be adjustable. Ideally, the settings should match measurements from real patient data. The

adjustments can be programmed to occur automatically based on basic patient data, so that the user does not have to manually configure all the settings. The simulator could then re-create a virtual model of a particular patient. Clinicians planning on performing the epidural can practice beforehand on a virtual model of the patient thereby reducing the learning curve during the procedure on the patient. The four common patient positions adopted during epidural insertion are sitting, sitting with lumbar flexion, lateral decubitus and lateral decubitus with lumbar flexion. These four common positions at least should be modelled in an epidural simulator to give a greater level of realism than static epidural simulators. Ideally, variable spine flexibility could be achieved by modelling 3D flexible spine vertebrae and extended to other positions to simulate difficult spinal anatomy. This may allow simulation of spinal conditions such as curvatures and rotations caused by kyphosis and scoliosis. These conditions cause difficulties in placing the needle due to unusually positioned landmarks. Also the accuracy of the forces in epidural simulators is a topic of recent discussion [7-9], so it is important that the forces required to insert a needle during simulation match those achieved in reality. Skills learned during this simulation can then be transferred to the actual clinical environment.

3. Modelling the needle insertion forces

Epidural insertion consists of a complicated interaction of many forces, needle position and intrinsic properties of the epidural equipment: a) Each tissue has various viscosity, elasticity, density and frictional properties. b) Bubbles of air in saline can compress. c) The method of insertion can vary depending upon needle inclination angle, paramedian angle, speed of insertion and twisting of the needle. d) Properties of the needle can vary, including the angle of the tip, tip type - side tipped or two-plane symmetric, needle gauge from 15-20 and width of the metallic walls in hollow needles vary. e) Plunger resistance is caused by friction on the inner syringe walls. f) The flow of saline is restricted by the funnel narrow opening of the syringe at LOR. g) The needle orifice can plug with tissue obstructing saline release.

Theoretically, a model can partition reaction force down into its individual constituents. The thumb applies force onto the plunger of the syringe and this force interacting with the frictional and resistive tissue forces contributes to the ‘resultant pressure’, see Figure 1. This pressure cannot escape so it causes the needle to push forwards. This causes the ‘reaction force’ which is equal and opposite to the applied force and comprised of several factors: a) The cutting force required for the needle tip to pierce the tissue. b) Friction caused by needle shaft resistance on the tissue. c) Static friction to get the stationary needle moving. d) Side compression force is caused by the surrounding tissues. e) Torque is caused by twisting of the needle. f) All of these forces, resistances and torque vary according to depth and tissue stiffness.

It is not feasible to measure all of these forces individually in-vivo and it would not make sense to measure the exact proportions of each force that make up the reaction force. In practice, it may be sufficient to measure the resultant pressure of the saline instead. Measuring resultant pressure provides a combination of all reaction forces, which is felt by

the anaesthetist during insertion, and this combination of all forces is what simulators need to re-create to simulate the feeling on insertion.

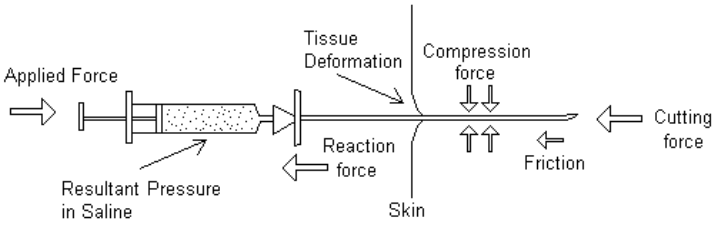

Figure 1. Several forces involved with needle insertion

4. Pressure measurement for realistic epidural simulation

A sterile wireless measurement device was developed to record the resultant pressure of the saline inside the syringe during an epidural needle insertion. This measurement device is used to enable data collection to quantify the pressure during the epidural procedure. Quantifying the pressure will enable accurate configuration of an epidural simulator.

Our novel pressure measurement device has wireless functionality and by using entirely sterile components allows in-vivo trials to be conducted with patients. A wireless data transmitter is utilized to minimize the equipment and disruption in the hospital room (Figure 2).

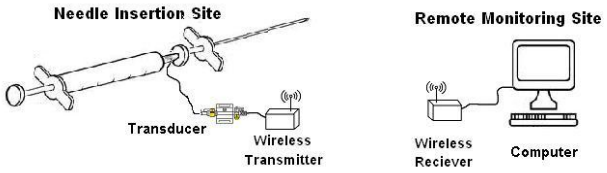

Figure 2. Remotely monitored wireless epidural pressure measurement system.

The design aims to minimise changes to the standard epidural set up. A small sterile three-way tap (BD Connecta™) is connected between the Tuohy needle and syringe (Figure 3). The tap is connected to the pressure transducer via a one metre length of saline-filled sterile manometer tubing. The transducer's electrical plug is connected by a short electrical cable to our wireless transmitter. At the remote site, a wireless receiver is connected via Universal Serial Bus (USB) to the computer.

The UTAH Medical Deltran disposable transducer is used for the pressure measurement sensor. These transducers are commonly used in hospitals to monitor systemic blood pressure and central venous pressure. Transducers produce a small electrical signal based on the pressure of the liquid inside the manometer tubing. Disposable transducers are designed to have accuracy of +/- 3% with the average output of 100.03 +/- 0.55 mm Hg and the worst cases being 98.53 and 101.36 when 100 mm Hg was applied [10].

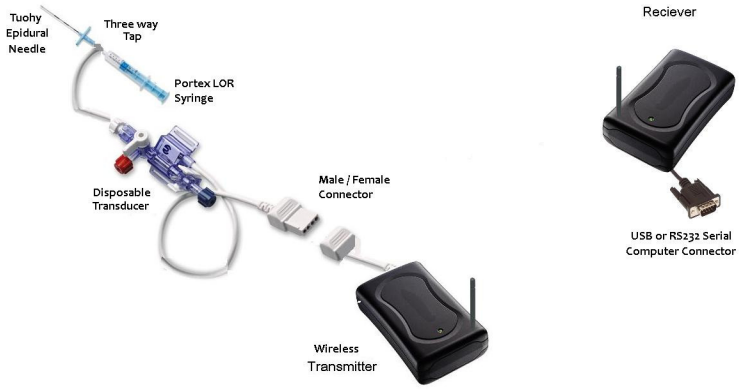

Figure 3. Wireless Device for recording measured pressure of saline during insertion.

The computer can process pressure data, display a real-time graph on screen and simultaneously record the data to a file. When the anaesthetist presses on the syringe plunger, the saline inside the syringe is pressurised and the device quantifies this pressure. The computer runs our custom built software (Figure 4) which monitors pressure data as it arrives [11]. The software displays the live data on screen in the form of a real-time graph, can save graphs as images to file and writes data to a text file. The data files can be used for further analysis using statistical software. Before each insertion, the graph and start-time are reset and a new data file is created. Pressure can be converted into various units. In the current implementation the pressure is measured in mmHg or kPa and also a provision is given to determine force on the plunger in Newtons. This directly provides actual pressure measurement of saline inside the needle as applied to a continuum. To test this device a pilot trial was conducted on a porcine cadaver.

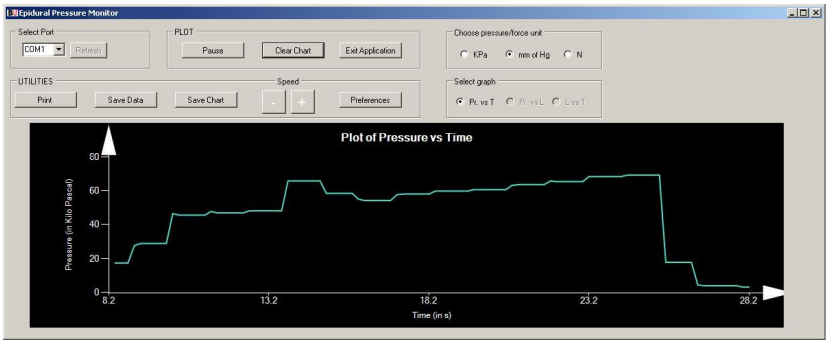

Figure 4. Screen print of the software to monitor and record pressure of saline during insertion

5. Trial on porcine cadaver

A trial using a section of a porcine cadaver was conducted to test the pressure measurement device during epidural insertions. The pig is claimed to be the closest animal model for

human spinal research and can be a representative anatomical model for the human spine and tissues [12]. The porcine tissue specimen was a double loin saddle cut. The cadaver was obtained from a livestock farm within 24 hours of slaughter without being frozen or modified in any way to avoid desiccation and deterioration of the spinal tissues which would affect the pressure measurements. The pig was a standard hybrid Large White cross Saddleback. The specimen contained the entire back in one piece, with the whole spine, and all tissue layers from external skin, through to the thoracic cavity. The porcine tissue was mounted vertically against a wooden support to mimic sitting position, resting upon, but not attached onto, a platform beneath (Figure 5).

Epidural insertions were performed by two experienced anaesthetists. The epidural space was located using a Portex 16-gauge Tuohy needle (Smiths Medical International Ltd, Kent, UK) at L2/3 or L3/4 intervertebral levels using a midline approach. Subsequently a number of different vertebral levels ranging from T12-L5 were targeted. The porcine spine was palpated to locate anatomical landmarks prior to insertion. The Tuohy needle with its introducer stylet penetrates the skin as is standard procedure. The recordings of pressure were then started and continuously recorded throughout needle insertion until after the loss of resistance had been experienced.

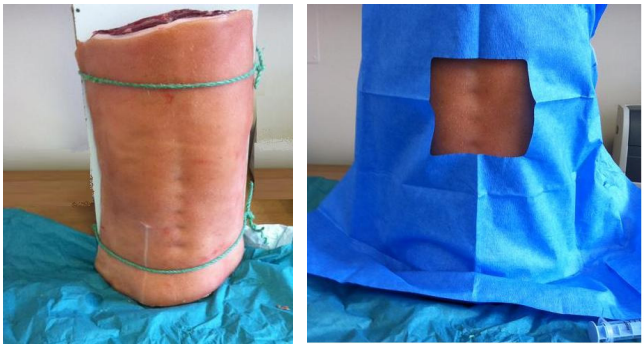

Figure 5. Porcine cadaver set up for Tuohy needle insertions

The majority of insertions located the epidural space during the first attempt. Data from hitting bone was also recorded to analyse the effect on pressure. In some cases, the number of attempts to find the space was greater than three so those recordings were abandoned. The maximum pressure during ligamentum flavum was 500 mmHg. The highest pressures were obtained when the Tuohy needle hit bone.

The results demonstrated that during needle insertion the saline pressure started low and gradually built up, although the increase was not entirely steady due to the various tissues encountered. A similar pressure trend was found; a depression occurred on insertion 2 during 3-6 seconds and insertion 3 during 12-15 seconds (Figure 6, circular area). This may have been caused by the interspinous ligament and the pressure required to traverse this was 350 mmHg on insertion 2 and 470 mmHg on insertion 3. The final peak pressure was 500 mmHg which was caused by the ligamentum flavum (Figure 6, rectangular area). It was

also noted that after the final drop of pressure there was often a 'step' before the bottom pressure was reached (square area). One explanation is that the initial pressure is the effect of opening up the epidural space which is a potential space and also saline pushing the dura away.

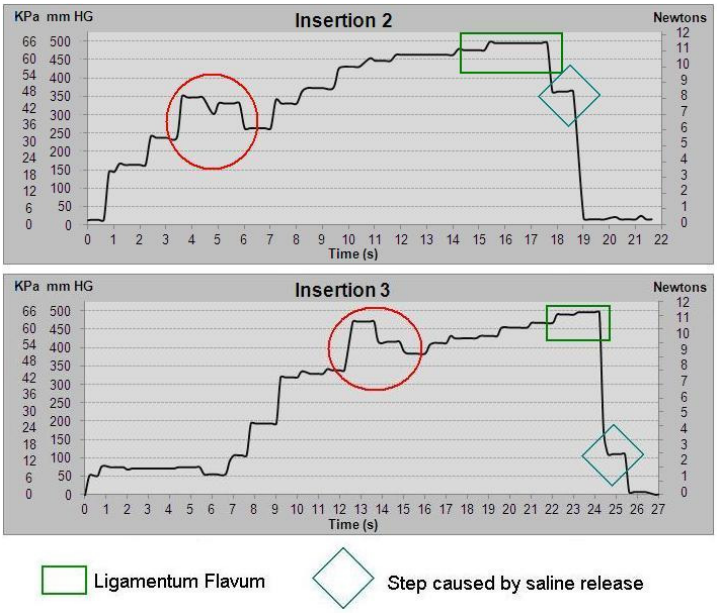

Figure 6. Pressure recordings durings two successful insertions to the epidural space.

The opinion of the trial anaesthetists was that porcine tissue did feel like a close approximation to human tissue and the shape of the graphs were similar to graphs previously reported from human insertions [8]. In most cases the resulting pressure-time graphs clearly show a drop when the loss of resistance occurred as the needle entered the epidural space (Figure 6). The maximum pressure peak during successful insertions ranged from 470 to 500 mmHg (62.7 - 66.7 kPa) caused by ligamentum flavum. After this the needle tip enters the epidural space causing a sudden loss of pressure back to the starting pressure. The shapes of each graph in successive trials were similar but also different to reflect individual variations.

The results of this pilot trial demonstrate that the wireless pressure measuring system is accurate and responsive in the porcine model. Such measurements from patients could be used to create realistic epidural simulators.

6. Image processing for non-contact needle depth measurement

The reason why needle depth is important is that it relates the depths at which each resultant pressure occurred during the epidural procedure. This can also provide

information about the depth of ligaments. We have developed image processing algorithms to measure the needle depth by a wireless camera during insertion [13].

During the epidural insertion procedure, the needle is slowly advanced through layers of tissue into the epidural space which is on average somewhere between 40-80mm deep. It is possible to record the depth of the needle tip by viewing the 10mm markings printed on the metallic needle; however, it is important to measure the needle depth precisely so that the needle travel can be guided with available measurements from techniques such as ultrasound scanning or magnetic resonance imaging for precise needle placement in the actual procedure. We have developed a novel image processing technique which aims to measure insertion depth of an epidural Tuohy needle in real-time. The implemented technique uses a single wireless camera to transmit depth data remotely to a host computer. Combining length and pressure data enables more accurate interpretation of the data in that the various changes in pressure can be linked to the actual depth at which the changes occurred.

The 16 gauge Portex Tuohy needle of 80mm length (Figure 7) is the most common epidural needle used in hospitals. The needle has grey and silver markings on the metallic shaft at 10mm intervals which are used by the software as a reference length. The blue handle is the plastic part at the base which is held by the operator and connected to a LOR syringe. This is used for colour detection.

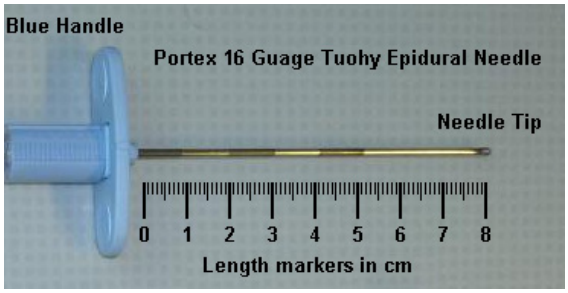

Figure 7. Properties of the 80mm Tuohy needle used for image processing

The actual technique of length and size measurement by digital image processing is well established, however, in this specific circumstance, image processing is much more complex and challenging due to many reasons; (i) the needle is a thin, narrow object, (ii) the needle is composed of reflective stainless steel, (iii) the needle is circular in cross-section causing colour changes around the shaft of the needle, (iv) wireless camera introduces transmission noises, (v) as the needle is tilted it reflects in different directions, (vi) the needle will not be the only object in the foreground due to the operator's hands and patient's back, (vii) lighting conditions vary from room to room. We have overcome these problems by advanced analysing techniques focusing on a small area of the dynamic environment.

The actual technique involves placing a wireless camera in the procedure room, one metre away from the needle insertion, which will transmit data to a remotely located computer.

The camera transmits a 640x480 pixel image in full colour over a 20MHz wireless link. The computer contains the image processing algorithm to detect the visible needle in the image and measure its length. The first step in the algorithm is to automatically calibrate the background model. For ten seconds, with no objects in the foreground, the colour values (HSV) for each pixel are analyzed. Maximum and minimum values are stored in an array and used later as a background model. HSV values from each frame are compared to the background model. Foreground objects are identified by HSV values outside of the expected range. The pixels from foreground objects are scanned for HSV values which match the blue handle. The centre point of the blue handle is found by taking an average and is stored for object tracking in subsequent frames, and is assumed to be approximately at the level of the needle shaft. The rightmost edge is stored and assumed to be the start point of the metal shaft. The blue handle is removed from further processing. The algorithm scans horizontally from the position of the blue handle to find the metal needle shaft by matching HSV values. The leftmost and rightmost pixels in the metal shaft are identified. These are stored for tracking in subsequent frames. At this point a strip of image remains over the needle. For each column, an average HSV value is taken. This average is used to create four separate histograms for H, S, V and the total along the length of the metallic shaft. The histograms identify sudden changes in colour, caused by the boundaries between 10mm markings (Figure 8). Histograms make the markings more detectable under reflective conditions. The number of visible 10mm markings is counted. The number of pixels in each division is counted to find how many pixels equate to 10mm. If the final marking is only partially visible the length is calculated by comparing it to a full division.

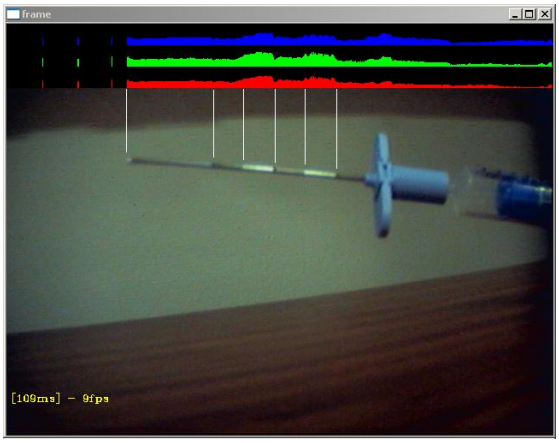

Figure 8. Output of the algorithm to measure needle length with histograms

The image processing algorithm was tested during insertions. The needle was successfully detected and measured accurately in most frames. The developed software was used to draw a graph of the length in real time and write the length data into a data file. Figure 9 shows the graph during an insertion in which the needle was slowly advanced and then rapidly withdrawn. We found that length measurement was accurate to within +/-3mm,

when the needle was 500mm from the camera. The graph shows two erroneous readings at about 4 and 8 seconds, which was due to camera noise and in these frames the needle shaft was not detected properly, but all other frames were successfully measured and verified by the actual measurement. The total insertion took about fifteen seconds with 10 frames per second. The failure rate was 3 frames out of 150 which gave an overall 97.8% reliability during this insertion [13]. Errors like this could potentially be removed by ignoring sudden jumps in the data. The graph currently displays length but this can be converted from length to needle depth by simply subtracting the value from 80 mm, which is the total length of the needle.

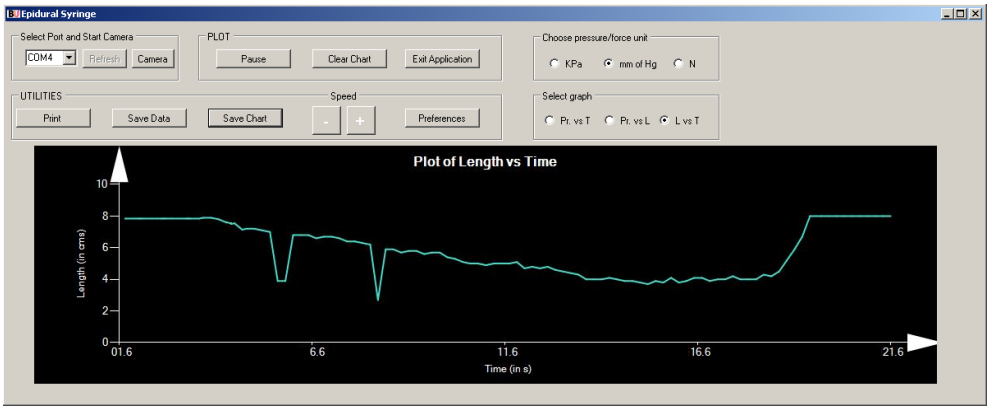

Figure 9. Software showing plot of needle length during insertion

The distance between needle and camera can be varied because length is measured using the 10mm markings as a reference length. At distances over 150cm the reliability dropped but this could be improved with a higher resolution camera. The needle can be tilted up or down to +/-30 without any adverse effect to measurements. Tilting towards or away from the camera does not affect measurement as long as the divisions are clearly visible because division length differentiates between length reductions caused by tilt and caused by insertion. Failures occurred on some frames, due to blur in the image, or at certain angles where silver and grey areas became merged. The background model successfully removed the majority of background, even with cluttered multi-colour backgrounds.

7. 3D spine modelling for epidural training

In order to simulate the whole epidural procedure a realistic user interface must be provided together with the flexibility of 3D visualization and haptic interaction. The 3D models for the epidural simulator were generated with an object modelling software. Each vertebra is an individual wireframe model, constructed from 514 vertices. The vertices are positioned and then wrapped by a texture. Shadows and light sources are applied through OpenGL interfaces. The spine in the simulator contains 26 separate objects for the thoracic, cervical and lumbar spinal vertebrae, sacrum and coccyx. Layers of tissue, fat, muscle and

skin were appended as layers above the bones. The different parts of the model were exported into separate format files. The format is text based with each vertex on a separate line. A custom C++ OpenGL graphics application then parses the text file to re-create each vertex. The epidural Tuohy needle was created as separate 3D models allowing it to be moved around independently. This is important to allow the operator to place the needle anywhere along the spine for training purposes.

The 3D objects can be viewed as stereograms (Figure 10) by displaying two images of the same object side by side with slight rotation around the Y axis [14]. The epidural simulator also supports this method of stereo in addition to page-flip stereo.

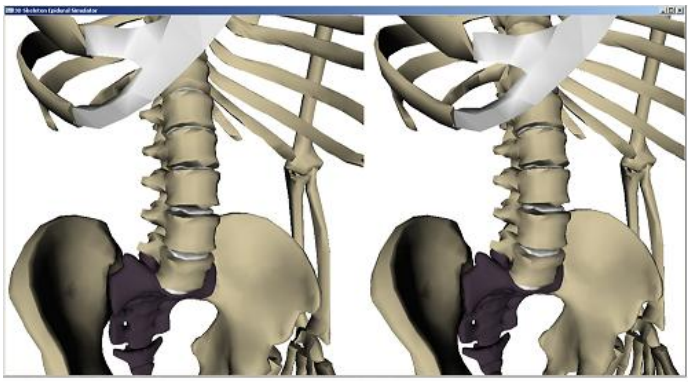

Figure 10. Stereogram view of the spine model with two perspectives and binocular parallax

Transparency is applied to skin, subcutaneous fat, supraspinous ligament, interspinous ligament and ligamentum flavum. This allows the user to see the position of the needle tip in the tissue layers. Transparency can be adjusted during the simulation by a control on the keyboard. Rotation is enabled allowing the camera angle to rotate around the scene. This is applied by OpenGL translation and rotation which gives an effect of camera movement whilst the other objects all remain stationary. During rotation, the tip of the needle remains at the central focus point of the screen. Zoom can be applied to move closer or further away from the site of insertion in the working epidural simulator. Pan can also be applied which is a translation of the camera which allows the user to view other areas or to move up and down the spine when selecting the insertion site.

Another issue equally important is the flexibility built into the spine model. There are four common patient positions adopted during the administration of spinal or epidural anaesthesia [15]. Lateral decubitus (Figure 11) involves lying down sideways on the patients left or right, usually the right side is used for caesarean patients, because it is the opposite side from which the patient will lie on during surgery in the left lateral tilt position, which helps to increase the spread of anaesthetic. When the patient lies in lateral positions their back should be close and parallel to the edge of the bed, with their spine in a straight line. However, a variation to this position, maximal lumbar flexion in the lateral decubitus position can be used. The sitting position is preferred and often required in obese patients to

enable the palpation of spinal processes and identification of the midline. Finally, the sitting position combined with maximal lumbar flexion is also used, and having the patient bend forward is advantageous to the anaesthetists because it increases the space between the vertebrae, which increases the target space for the needle to pass through.

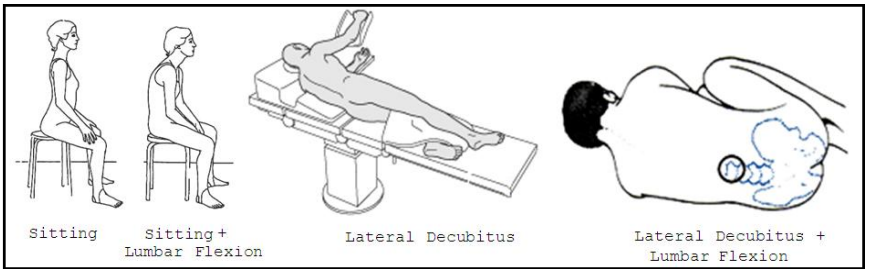

Figure 11. Four common patient positions used for epidural insertion

Based on this, the patient could bend the spine to various positions, so the epidural simulator is required to use computer graphics models of the human spine which can bend, flex and twist. The model can realistically duplicate the shape of the spine during various sitting positions adopted by patients during surgery and epidural anaesthesia. The extent of bending and flexing is kept within the limits of human spine flexibility. Also the model vertebrate adapt in size to match weight and height of specific patient bodies based on parametric modelling [16]. Our spine model is flexible for epidural simulation which offers accurate models of spinal vertebrae.

The human spine consists of twenty six vertebrae. Each of the vertebrae connects with numerous ligaments. Internally, there is a protective space running through the centre of the spine, housing the spinal cord. The column of vertebrae also provides connection points with the ribs and back muscles. The twenty six vertebrae are segmented into five regions, each with varying characteristics. From cranial to caudal there are cervical vertebrae (C1-C7), thoracic vertebrae (T1 – T12), lumbar vertebrae (L1 – L5), sacrum and coccyx. The human spine is able to bend, flex and rotate in various directions. Lumbar flexion occurs when the patient bends forwards and lumbar extension occurs when bending backwards. The spine was modelled using 3D design software, formed from 26 individual vertebrae, shown in Figure 12. The 26 vertebrae were each loaded as 3D models into a custom made software graphics application. The software renders 3D objects using vertices with the OpenGL graphics library and its utility toolkit (GLUT). The colours of each region of vertebrae bone, flesh and the spinal discs were set using materials.

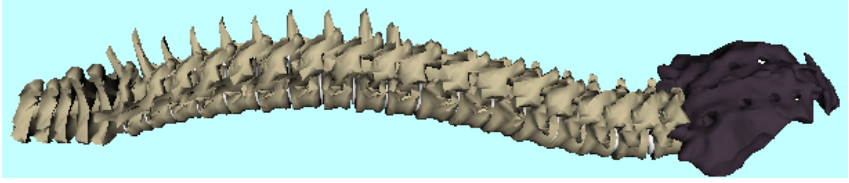

Figure 12. The model spine consisting of 26 individually rendered 3D vertebrae

Initially the vertebrae are positioned in the standing position and are then adjusted by mathematical equations to match the current patient position. The curvature of the spine for four common patient positions was calculated using the equations. The shape of the spine was based on the four common patient positions used for epidural insertion. Our model's prediction for the spine shape for each of the positions is shown in Figure 13 [14].

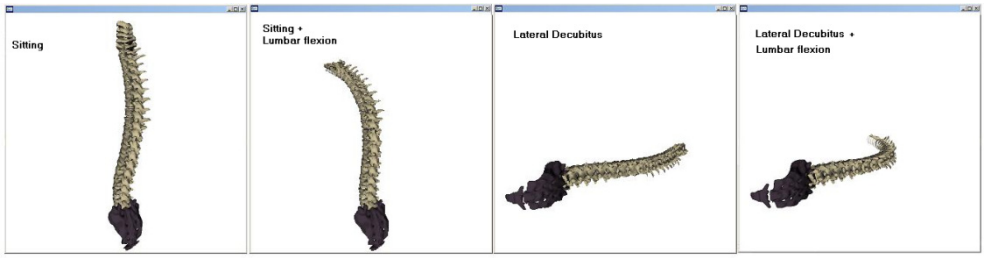

Figure 13. The spine model with flexion for four common patient positions

The ability to flex and rotate the spine has provided the opportunity to simulate epidural insertions on patients in various positions. This is important because the feeling of insertion is different for each patient position. This novel aspect has not been attempted in epidural simulation before and will increase versatility of the simulation.

8. Heterogeneous ligament modelling

Since the introduction of traditional computer graphics and modelling techniques, the primary focus has been to display and modelling of homogenous objects which have uniform interior and consist of one material throughout. This was acceptable for many situations, however, such surface-based approaches were aimed to represent the visual appearance of the external layer of objects, leaving the interior untouched. Recently, with the availability of increased computing power, the focus has shifted from surface-based to volume-based graphics, whereby volume-based architecture attempt to describe the material structure of internal regions by the use of voxels [17]. This can allow manipulation and experimentation on the physical properties of the materials, such as density, friction, elasticity, tensile strength and in so doing opens up new possibilities for experimentation. Heterogeneous objects are a step further, being solid physical objects, which consist of two or more material primitives but offering the advantage of materials that may be distributed continuously blending with each other.

For epidural needle insertion, the needle passes through several ligaments along its path to the epidural space, with each of the ligaments having different properties such as density, resistance to insertion and friction (see Section 3). A model is required to encompass these aspects of each ligament if the graphics are to be capable of displaying a true likeness of the materials in-vivo. Ligamentum flavum (LF) is heterogeneous in nature, containing both elastic tissue and fibrous tissue. Certain data describing the ligamentum flavum has been recorded in the literature and can be used to set up a heterogeneous model of the ligament.

As LF thickness increases, fibrosis increases and elastic tissue decreases. The dorsal side of LF contains more fibrous tissue and less elastic tissue than the dural and middle sides, as indicated by a fibrosis Score of 1.58, 1.63, and 2.63 for dural, middle, and dorsal sides respectively [18]. The loss of elastic fibres caused by increased thickness is more pronounced along the dorsal side. A single patient has several ligamentum flava, one at each spinal level between the lamina and their thicknesses vary according to the spinal level. A study of 77 patients measured LF at spinal level L2/3, L3/4, L4/5, and L5/S1, the mean LF thickness is 2.41, 3.25, 4.08, and 2.68 mm [18]. It was shown that the thickest part of ligamentum flavum is consistently at L4/5, which is the level that endures the greatest mechanical stress. LF is crescent shaped in cross section on the horizontal plane with the thickest part in the middle. It wraps around the circular epidural space and dura. It connects to lamina above and below. The elastic fibres are yellow in colour, hence 'flava' being Latin for yellow. Each flava is a separate ligament which is clearly seen from the side of the lamina.

Object modelling software was used to create a model of the vertebrae. At the location of L2/L3 a ligamentum flavum was modelled with the thickness 2.41mm which was internally comprised of bundles of fibres (Figure 14).

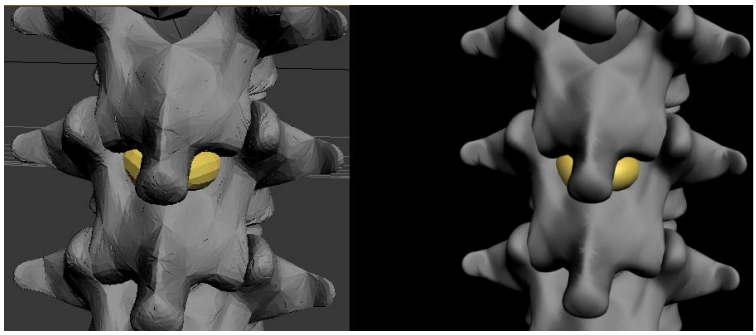

Figure 14. The modelled ligamentum flavum between L2/L3 vertebrae.

The interior structure of the ligamentum flavum has been modelled by numerous bundles of fibres extending vertically and parallel to one another, as do the elastic and fibrous tissues in-vivo. By creating this heterogeneous model of the internal structure of ligamentum flavum, the model will describe more accurately how the material responds to a needle being inserted through it. Similar models may be created for interspinous ligament and supraspinous ligament which are also both heterogeneous in nature, consisting of over three types of elastic fibres that can used to provide realistic haptic feedback.

9. 3D visualisation of epidural procedure

We have applied stereoscopic 3D computer graphics for visualization of epidural insertions. The stereoscopic images are viewed through a head mounted visor containing two OLED micro-displays in stereo using the page-flipped method. The 3D graphics are built from several vertex models of the anatomical structures as described in section 7. The stereo

simulation allows depth to be perceived so that the operator can judge depth of the needle tip in relation to tissue layers and bones, which aids to the location of the epidural space. Applying stereoscopic vision to epidural simulators helps the operator to visualize the depths required for correct needle placement in the epidural space [14].

Depth judgement is crucial to the technique and since stereographics allows the perception of depth in 3D graphics, epidural simulators can benefit greatly from stereo-technology. Here the aim is to apply stereo vision technology to simulate epidural needle insertion. Without stereo graphics the depths of objects in simulations are not perceived accurately. By viewing 3D graphics on a flat computer screen there is no way of knowing the actual distance between objects other than by estimating their size. Estimation is not always accurate and some medical applications may require far more precision in depth perception. Epidural simulators require the needle tip to penetrate several layers of tissue between 42-47mm thick and must stop within the 6mm epidural space [19], which is difficult to achieve without depth perception. With stereo vision, distance can be perceived natively allowing the user to intuitively view the depth and distance between objects by perceiving differences between the two images, if images are appropriately scaled.

Stereo glasses contain two small OLED screens, one for each eye. Alternatively, glasses can be polarized, which allows viewing of a polarized screen, which has both images superimposed, one of which arrives at each eye. Shutter glasses can be used which contain moving mechanisms to consecutively close each eye similar to a camera shutter. The screen then displays images for left and right eye consecutively at the same shutter speed. Alternatively, a glasses free approach, vertically dispersive holographic screen (VDHS) can be used by directing two beams of light containing the images into each eye separately [20]. Mirror screens contain two monitors mounted at 110 degrees with a plane of silver-coated glass combining the two images and cross-polarized glasses are worn to separate the images. For all stereo systems, once the two images arrive separately at each eye, the brain combines them to generate 3D with depth perception based on some calibrated data.

For this epidural simulator, we have used stereo glasses containing two OLED micro-displays, one for each eye, with magnifying lenses. Figure 15 shows how the epidural simulator is being used with the stereo glasses displaying the 3D spine model. The glasses have advantages that the user can see the image whichever direction they look in and as they turn their head motion detectors can rotate the image to follow. The glasses produce a 40-degree diagonal field of view for each eye. The image appears the same size as a 105 inch projection screen viewed from 12 feet. Magnifying lenses allow the eye to focus further away avoiding eye strain. The graphic resolution must be fixed at 800x600 pixels which display sufficient details. Two separate images are displayed on each eye display. Stereo is achieved by using the page-flip method. A signal is generated by the graphics card at 60Hz, with the images consecutively swapped between left eye and right eye. The swapping is done by the graphics card drivers. The hardware inside the 3D glasses splits this into two separate 30Hz signals and delivers one to each eye, this results in stereoscopic images.

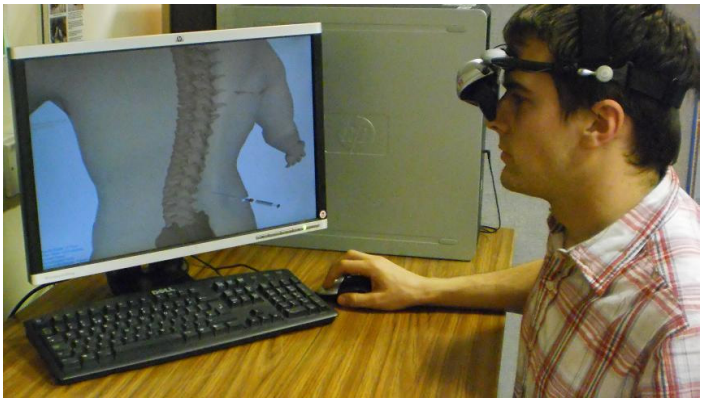

Figure 15. Stereo glasses used for epidural insertion visualization

The epidural simulator software interfaces with head motion detectors. When the user turns their head, the 3D objects rotate by the same degree in the opposite direction to create an illusion of camera rotation. This interface allows the user to change the view point to different directions by turning their head, so that the mouse and keyboard are no longer required. The feedback from experienced anaesthetists suggested that the flexible spine model will be useful for modelling patient position. The options for adjustable body shape and size was seen as a positive step to encapsulate the variety of patients which has not previously been accomplished.

10. Haptic interface for epidural insertion

Haptic devices have become a more popular and accepted tool for medical simulation and provide an accurate way of re-creating the feel of surgery [21, 22]. The insertion of an epidural is a procedure which relies almost entirely upon feeling the forces on the needle. Epidural simulators are therefore ideally suited to haptic technology. This section describes methods for configuration of a haptic device to interact with 3D computer graphics as part of a high fidelity epidural simulator development program.

Haptic devices have been used in epidural simulators previously, although they are not based on measured patient data from needle insertions. Instead, they are configured by 'experts' trialling and adjusting the system. It is therefore hard to assess the accuracy of the forces generated and so creates a real potential for improvement. The haptic device has currently been set up to reconstruct the force data found during the porcine trial. The force data from the graphs were divided into sections to represent each of the tissue layers separately [23].

A haptic device has been connected and used as an input to move the needle in 3D, and also to generate force feedback to the user during insertion (Figure 16). A needle insertion trial was conducted on a porcine cadaver to obtain resultant pressure data (Section 5). The data generated from this trial was used to recreate the feeling of epidural insertion in the simulator. The interaction forces have been approximated to the resultant force obtained during the trial

representing the force generated by the haptic device. The haptic device is interfaced with the 3D graphics (see Sections 7-9) for visualization. As the haptic stylus is moved, the needle moves on the screen and the depth of the needle tip indicates which tissue layer is being penetrated. Different forces are generated by the haptic device for each tissue layer as the epidural needle is inserted. As the needle enters the epidural space, the force drops to indicate loss of resistance. An advantage to the use of haptic devices for epidural simulators is that they can accept various adjustable settings, so that patient variation including weight, height, age and sex can be accounted for, which helps to train for a range of patients. Patient variety is becoming an even more important aspect than ever since the current obesity epidemic poses great challenges for the anaesthetist. In obese patients, the depth to the epidural space is increased, anatomical landmarks are harder to feel and the midline is more difficult to locate. The resultant effect is that the risk of injury is increased.

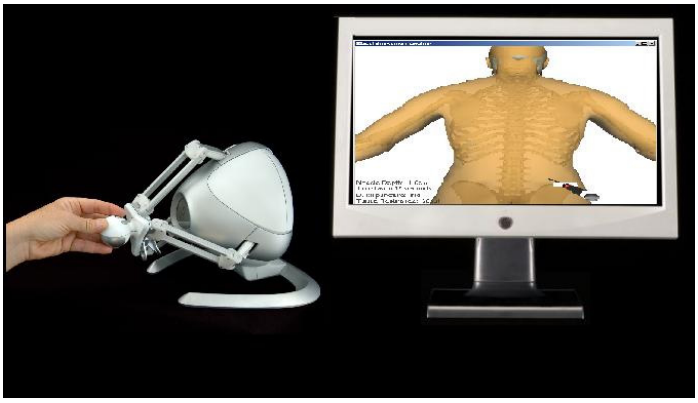

Figure 16. The haptic device interfaced with the graphics

To apply different forces to each layer, 3D vector regions were defined within the graphics model. As the needle tip enters these regions, the software identifies which tissue layer the needle is in, based on the depth data from the trial (Table 1). The software then uses a lookup table to find the appropriate force for each layer, and instructs the haptic device to generate that force. The forces generated represent the resultant pressure on the syringe which is a sum of all resistances to insertion, which are the equal and opposite to the force applied by the user. For example, if a particular layer has insertion force of 4.3N, and the user is pressing with only 3.2N, then the haptic device exerts 3.2N, so the stylus remains stationary. Only if the user increases the force to over 4.3N the stylus will move forward. Table 1 is based on measurements taken from our porcine trial in line with [24].

The haptic device is also able to simulate palpation of the lumbar region. Palpation is the process for choosing which location to insert the needle. The haptic device was configured for palpation by creating a surface hardness profile of the lumbar region, with a hardness value for each point in the region (see Section 8). The haptic device can be used to press at any point and the user can feel the hardness at that point. This allows the user to locate landmarks and choose a point to commence needle insertion. Our advanced haptic interface is based on the

measured data and the aim is to develop a generic simulator based on measured data to offer a realistic in-vitro experience before attempting the procedure on actual patients.

Porcine Tissue Layer	Tissue thickness (mm)	Needle depth (mm)	Insertion force (N)
Skin	3	0	12.9
Subcutaneous fat	6	3	6
Supraspinous ligament	4	9	9
Interspinous ligament	26	13	8
Ligamentum flavum	3	39	11.1
Epidural space	6	42	0
Dura	15	48	2.0

Table 1. Insertion forces in porcine [23, 24]

11. Human-computer interface for loss of resistance syringe

With the above developed components, a hardware device has been created consisting of a regular Portex LOR syringe connected to the computer via a serial data transfer device. This allows a regular clinical syringe to be used as part of an interactive system for the epidural simulator development. The syringe was also combined with the haptic device to create a comprehensive human-computer interface. The simulator can measure force applied to the plunger and the resultant pressure of the saline inside the syringe barrel. This interface enables a real clinical syringe to interface with a 3D graphical visualization showing the simulated insertion of the Tuohy epidural needle through the spinal ligaments.

The developed hardware interface makes use of the equipment as developed in Sections 4 & 6 by incorporating custom made hardware with the developed software and the graphical visualization of the needle insertion procedure. The hardware device takes measurements of the forces applied onto the needle and the resultant pressure of the saline inside the barrel of the syringe caused by the pressure from the operators thumb on the plunger. The measurements are sent to the computer by a custom-made hardware interface device (see Sections 4 & 6). The graphical simulation uses these measurements to update the needle in the simulation and calculates the needle position. The graphical software calculates if any collisions have occurred between the needle and any bone structures, plus the resistance of insertion to saline, and the force required for the needle to move forwards through the current ligament.

The developed human-computer interface uses an actual syringe and an epidural Tuohy needle as shown in Figure 17. During insertions, the LOR syringe is normally connected directly onto the Tuohy needle. We have introduced a three-way tap between the needle and syringe. This connects onto a one metre length of saline manometer tubing which runs to a disposable pressure transducer. The transducer converts the pressure of the saline into an electrical signal. The electrical signal is connected into a hardware device which amplifies and sends the pressure reading to the computer. This allows the graphics visualization to

update according the pressure applied by the operator's thumb on the plunger of the syringe. This has the advantage that the user can control the visualization with the same equipment that would be used in-vivo, which is a more natural interface than simply using keyboard or mouse. Additionally, since the saline line separates the hardware device from the needle, the user can move the needle around since it is attached only by the saline line.

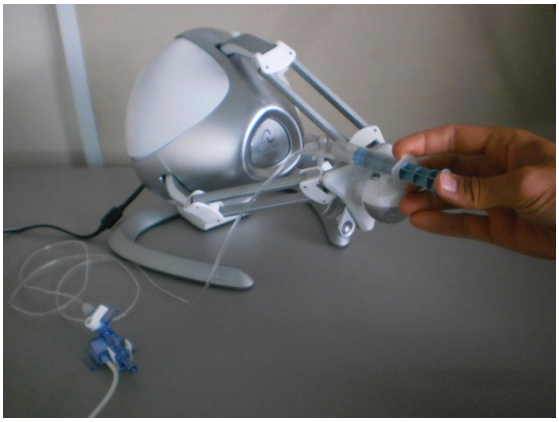

Figure 17. The syringe connected to the computer as an input device.

The hardware device runs at 8MHz. Data is transmitted from the hardware device to the computer using the serial RS232 port. The serial bit rate is running at 22000 bits per second. The serial data transfer protocol uses -12V DC as a positive bit and +12V DC as a negative bit. The serial transfer cycle starts with a negative start bit, followed by 8 data bits sent consecutively and finished with a positive stop bit. As shown in Figure 18, the following start bit can then occur either immediately or after a pause of arbitrary length.

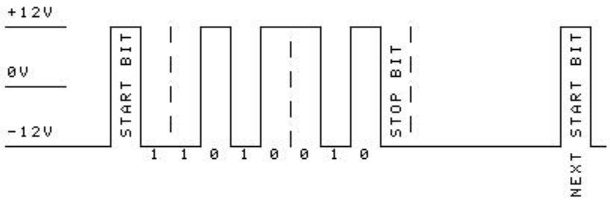

Figure 18. Binary serial data transfer protocol.

The 8 data bits are received and interpreted as binary and converted into a decimal number from 0 to 255 for use in the software. The decimal value represents the pressure of the saline between 0 to 70 kPa, which is 0 to 550 mmHg. The 256 possible values give an accuracy resolution to within +/- 0.14 kPa. This can be easily increased to 1024 with 10 bits data transfer which will then provide accuracy of within +/- 0.03kPa. The speed could also increase beyond the current 22000 bits per second but it does not seem necessary since no delay is noticed between pressing the plunger and seeing the results on screen. Currently at 22000 bits per second the time delay between bits is 45μS so the start bit is identified by

testing the pin for +12V, and then checking again after 22μS for the same high value. The computer runs the custom designed software which monitors the data as it arrives. Also the values are received by the graphics application which updates the visualisation to match the pressure applied on the physical syringe.

This study has demonstrated the development of a human-computer interface based around a clinical Portex LOR syringe connected via a custom made hardware interface device to a computer for use in an epidural simulator. The results show that the device is both fast and accurate enough to be used seamlessly in the simulation. The addition of the Portex LOR syringe with a pressure monitoring device has undoubtedly improved the human-computer interaction. Using the actual medical components in the implementation is beneficial because epiduralists will be familiar with the syringe and use it to interact with the 3D graphics visualization intuitively. The interface could be modified to be bi-directional i.e. the graphics software could send back data to the device which could control a motor to cause forces which affect the physical needle so that the user can feel the forces through the needle as in-vivo.

12. Creation of a novel epidural simulator

The presented biomedical engineering ideas have enabled us to develop a simulator with a combination of engineering, computing and clinical technologies as discussed in previous sections above. Data from the developed measurement devices have been used to configure a realistic force feedback epidural simulator [25]. Numerous improvements have been identified that could enhance existing epidural simulators. Manikin models are generally static and only able to represent one or two patient variations, such as normal and obese. An advanced simulator would be able to simulate insertions on a variety of body mass indices because excess fat deposition has the potential to generate very different changes in patient characteristics.

The developed system offers a virtual reality based epidural simulator (Figure 19) incorporating a 3D graphically modelled spine complete with skin, fat and tissue layers, supraspinous, interspinous ligaments and ligamentum flavum. In the current prototype, a Novint Falcon haptic device is used in combination with a Portex LOR syringe connected as a human-computer interface via a custom made electronic serial interface. As the haptic stylus is moved, the needle follows on the screen in 3D in real time. When pressure is applied to the plunger by the operator's thumb, this is displayed in the graphic model. As the needle is advanced through the tissues, the forces are generated by the haptic device to reconstruct the feelings of needle insertion through each tissue layer. The forces of the needle insertion are based on the recorded forces measured during the clinical trial, and this data based approach is more accurate than previous simulators which have used a user evaluation approach to configure the forces.

Novel aspects of our epidural simulator include stereo graphics, modelled vertebrae, spine flexibility, patient variation, haptic force feedback based on measured needle insertion data, custom made syringe interface. The simulated needle can be inserted at any spinal position

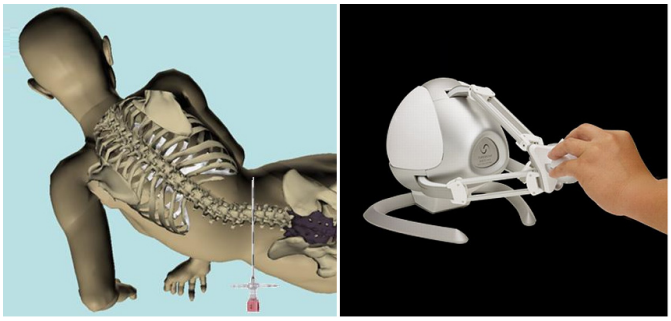

Figure 19. Prototype 3D graphics epidural simulator with haptic device interface

from T2 – L5 and needle direction from midline to paramedian. The 3D graphics allow a close-up real time view of the needle internally during insertion. The virtual patient can adjust to various body shapes, weights and heights since body size considerably affects insertion force. These all have roots in biomedical engineering that can potentially enhance many clinical procedures.

13. Conclusions

The application of biomedical engineering approaches can help simplify many clinical problems as demonstrated for the epidural procedure.

We have described in this chapter, the developed measuring devices which have successfully recorded the data on resultant pressure and depth of epidural Tuohy needles during insertions in a porcine model. These data are very useful in developing a realistic high fidelity epidural simulator. We aim to measure pressures in-vivo with obstetric patients in labour of differing body mass indices and integrating this data with ultrasound and MRI scan imaging data. It is our belief that the resulting epidural simulator based on such data will replicate the in-vivo procedure more accurately since it is going to be based on patient specific information. No such simulator exists at the present time.

The overall benefits of applying biomedical engineering techniques to this research are that we are able to achieve a high degree of accuracy and improved technology for replicating the epidural procedure. By achieving higher realism and accuracy of simulation, epiduralists will be better trained with the procedure and this in turn will improve patient safety by minimizing the risk of failure and harm to patients.

Author details

Venketesh N. Dubey and Neil Vaughan
School of Design, Engineering and Computing, Bournemouth University, Bournemouth, UK

Michael Y. K. Wee and Richard Isaacs
Department of Anaesthesia, Poole Hospital NHS Foundation Trust, Poole, UK

14. References

[1] Dogliotti AM. Research and Clinical Observations on Spinal Anesthesia: With Special Reference to the Peridural Technique. Anesthesia and Analgesia 1933;12:59–65.

[2] Carvalho JCA. Ultrasound-Facilitated Epidurals and Spinals in Obstetrics. Anesthesiology Clinics 2008;26:145–158.

[3] Wilson JG, Pallotta OJ, Reynolds KJ, Owen H. An epidural injection simulator. World Congress on Medical Physics and Biomedical Engineering, Sydney. 2003.

[4] Mayooran Z, Watterson L, Withers P, Line J, Arnett W, Horley R. Mediseus epidural: full-procedure training simulator for epidural analgesia in labour. Proc. SimTecT Healthcare Simulation Conference 2006.

[5] Magill JC, Byl MF, Hinds MF, Agassounon W, Pratt SD, Hess PE. A novel actuator for simulation of epidural anesthesia and other needle insertion procedures. Simul Healthc 2010;5(3):179-84.

[6] Dang T, Annaswamy T, Srinivasan M. Development and evaluation of an epidural injection simulator with force feedback for medical training. Stud Health Technol Inform 2001;81:97-102.

[7] Vidal FP, John NW, Healey AE, Gould DA Simulation of ultrasound guided needle puncture using patient specific data with 3D texture and volume haptics. Comp Anim Virtual Worlds 2008;19:111-127.

[8] Tran, D, Hor, K, Kamani, A, Lessoway V and Rohling, R. Instrumentation of the loss-of-resistance technique for epidural needle insertion, IEEE Transactions on Bio-Medical Engineering, 56(3), 2009, pp.820-7.

[9] Abolhassani, N Patel, R Moallem, M. Needle insertion into soft tissue: A survey. Medical Engineering & Physics 2007;29(4):413-431.

[10] Gardner, R. Accuracy and reliability of disposable pressure transducers coupled with modern pressure monitors, Critical Care Medicine, 24(5), 1996, pp.879-82.

[11] Vaughan N, Dubey VN, Wee MYK, Isaacs R. Measuring Tuohy Needle Insertion Force on a Porcine Spine, IEEE 6th International Conference on Bioinformatics and Biomedical Engineering (iCBBE 2012), 17-20 May, Shanghai, China.

[12] Busscher, I, Ploegmakers, JJ, Verkerke GJ. and Veldhuizen, AG. Comparative anatomical dimensions of the complete human and porcine spine, European Spine Journal, 19, 2010, pp.1104-1114.

[13] Vaughan N, Dubey VN, Wee MYK, Isaacs R. Epidural Needle Length Measurement by Video Processing, The IET Image Processing Conference 2012, 3-4 July, London.

[14] Vaughan N, Dubey V, Wee M, Isaacs R. Virtual Reality based Enhanced Visualisation of Epidural Insertion, ASME 2012 International Design Engineering Technical Conferences & Computers and Information in Engineering Conference, DETC2012-70951, August 12-15, 2012, Chicago, IL, USA.

[15] Chestnut DH. Obstetric anesthesia: principles and practice: 2009.

[16] Kasap M, Magnenat-Thalmann N. Skeleton-aware size variations in digital mannequins. The Visual Computer 2011;27:263–274.

[17] Pasko, A., Adzhiev, V. and Comninos, P., Heterogeneous Objects Modelling and Applications, 2008, Springer, Germany.
[18] Sairyo, K, Biyani, A, Goel, V, Leaman, D, Booth, R, Thomas, J, Gehling, D, Vishnubhotla, L, Long, R, Ebraheim, N. Pathomechanism of Ligamentum Flavum Hypertrophy: A Multidisciplinary Investigation Based on Clinical, Biomechanical, Histologic, and Biologic Assessments, Spine. Issue: Volume 30(23), 1 December 2005, pp 2649-2656.
[19] Cheng, PA. 1963, The anatomical and clinical aspects of epidural anesthesia, Anesthesia and Analgesia; 42(1), pp. 398–406.
[20] Magalhães, DSF, Serra, RL, Vannucci, AL, Moreno, AB, and Li, LM. 2012, Glasses-Free 3D Viewing Systems for Medical Imaging, Optics and Laser Technology, 44(3), pp. 650-655.
[21] Coles, T. R, Meglan, D, and John, N. W. 2011, The Role of Haptics in Medical Training Simulators: A Survey of the State of the Art, IEEE Transactions on haptics, 4(1), pp. 51–66.
[22] Halvorsen, FH, Elle, OJ, and Fosse, E. 2005, Simulators in Surgery, Minimally Invasive Therapy and Allied Technologies, 14(4), pp. 214-223.
[23] Vaughan N, Dubey VN, Wee MYK, Isaacs R. Haptic interface on measured data for epidural simulation, ASME 2012 International Design Engineering Technical Conferences & Computers and Information in Engineering Conference DETC2012-70891, August 12-15, 2012, Chicago, IL, USA.
[24] Hiemenz, L, 2001, Force models for needle insertion created from measured needle puncture data, Medicine meets virtual reality, pp. 180-6.
[25] Vaughan N, Dubey VN, Wee MYK, Isaacs R. Advanced Epidural Simulator with 3D Flexible Spine and Haptic Interface, DMD2012-6837, ASME Design of Medical Devices Conference (DMD 2012), 10-12 April, Minneapolis (USA).